RESEARCH ARTICLE

Figures and figure supplements

Downregulation of glial genes involved in synaptic function mitigates Huntington's disease pathogenesis

Tarik Seref Onur *et al*

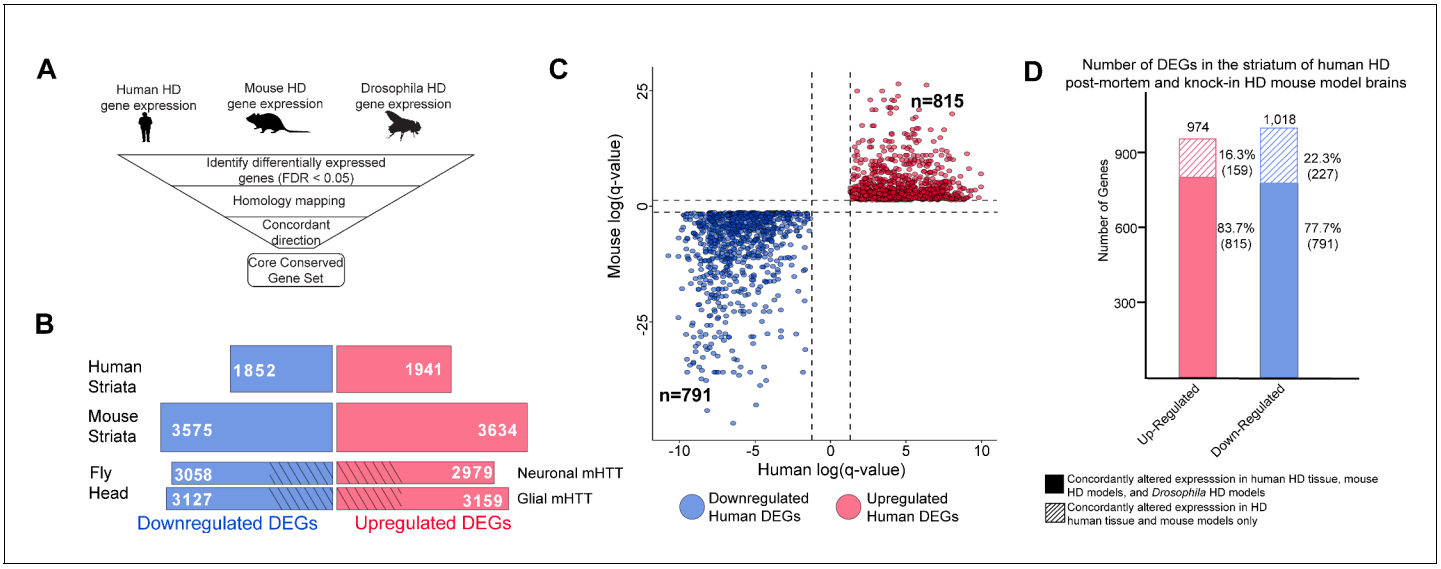

Figure 1. Differentially expressed genes (DEGs) in Huntington's disease (HD) human striatal tissue are concordantly altered in mouse and *Drosophila* HD models. (**A**) Our approach to identifying orthologous genes in tissues from humans, mice, and *Drosophila* with concordant expression changes (i.e., upregulated or downregulated in all three systems) following mutant *Huntingtin* (m*HTT*) expression. (**B**) The number of DEGs in each species-specific dataset that are downregulated (blue) or upregulated (red) (see Materials and methods). *Drosophila* DEGs were from flies expressing either the N-terminal ($HTT^{NT231Q128}$) or full-length m*HTT* (HTT^{FLQ200}) in neurons (*elav-GAL4*) or glia (*repo-GAL4*). The DEGs in flies are grouped according to the cell type expressing m*HTT* rather than the mHTT model. The cross-hatched regions of the *Drosophila* bars represent DEGs shared between the neuronal and glial sets: 1293 downregulated genes and 1181 upregulated genes. (**C**) Points in the scatterplot represent human DEGs identified by the strategy outlined in (**A**) that are concordantly dysregulated across all three species. Red nodes represent upregulated DEGs (n = 815), whereas blue nodes represent downregulated genes (n = 791). The overlap of these concordant DEGs represents approximately 40% of genes with altered expression in the human HD transcriptome that are upregulated ($p=6.37\times10^{-158}$) or downregulated ($p=1.66\times10^{-165}$). The p-value was calculated using a random background probability distribution over 2×10^5 random samplings. (**D**) The stacked bar graph highlights that a large majority of concordant DEGs in human HD striata and knock-in HD mouse models are also concordantly altered in *Drosophila* models of HD.

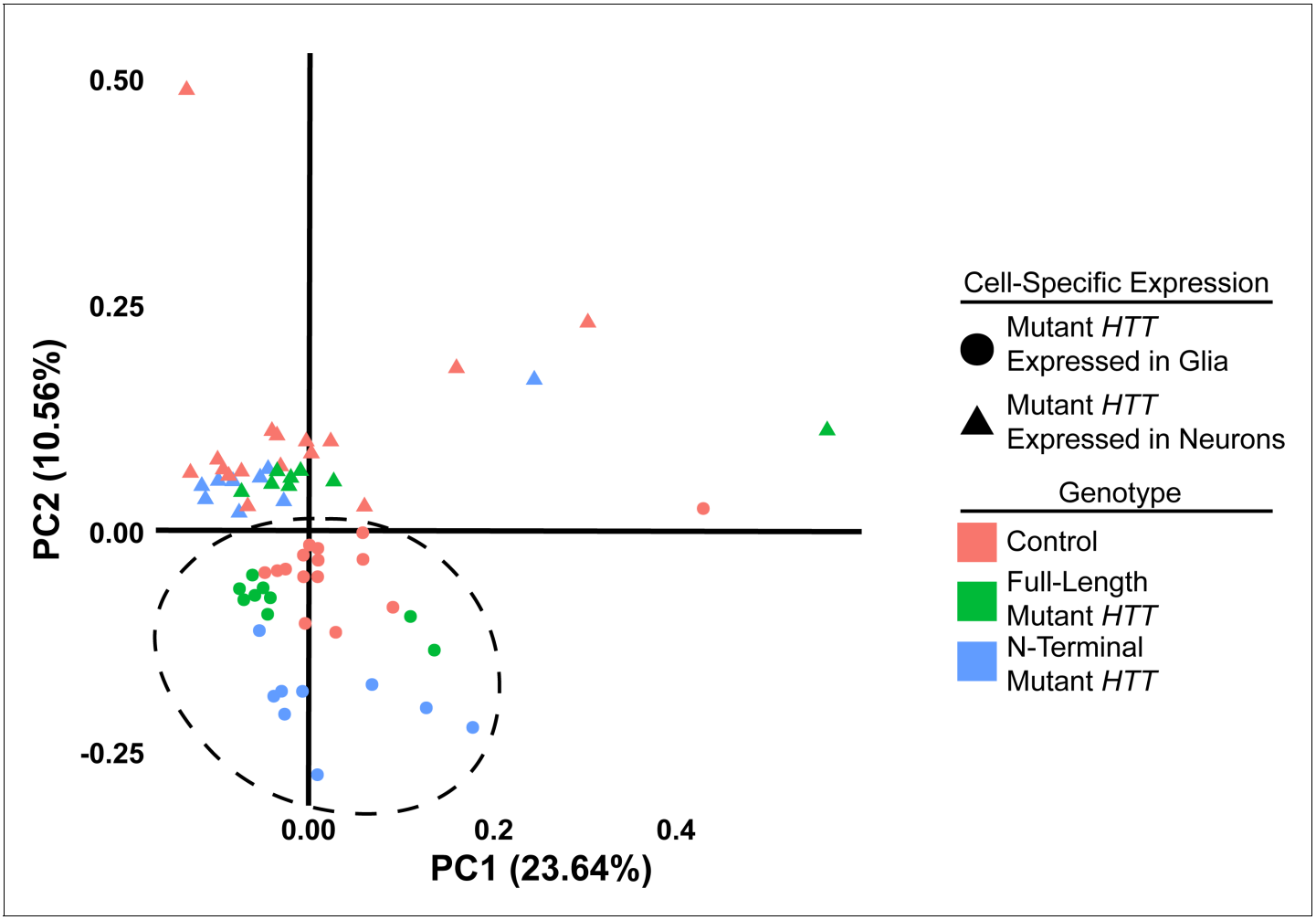

Figure 1—figure supplement 1. Expressing mutant Huntingtin (mHTT) in *Drosophila* glia or neurons leads to distinct gene expression profiles. In contrast, the full-length and N-terminal models show relatively similar gene expression profiles. Principal component analysis (PCA) plot of RNA-sequencing samples. Circles represent samples with transgenic expression in glia (*repo-GAL4*), while triangles represent samples with transgenic expression in neurons (*elav-GAL4*). Red points represent control w^{1118} controls, green points represent animals expressing the full-length protein m*HTT* transgene (HTT^{FLQ200}), and blue points represent animals expressing the N-terminal m*HTT* fragment transgene ($HTT^{NT231Q128}$). Outliers skew the first component on the x-axis (23.64% of the variability). Samples expressing m*HTT* in glia separate from those expressing it in neurons along the second component on the y-axis (10.56% of the variability; dashed circle).

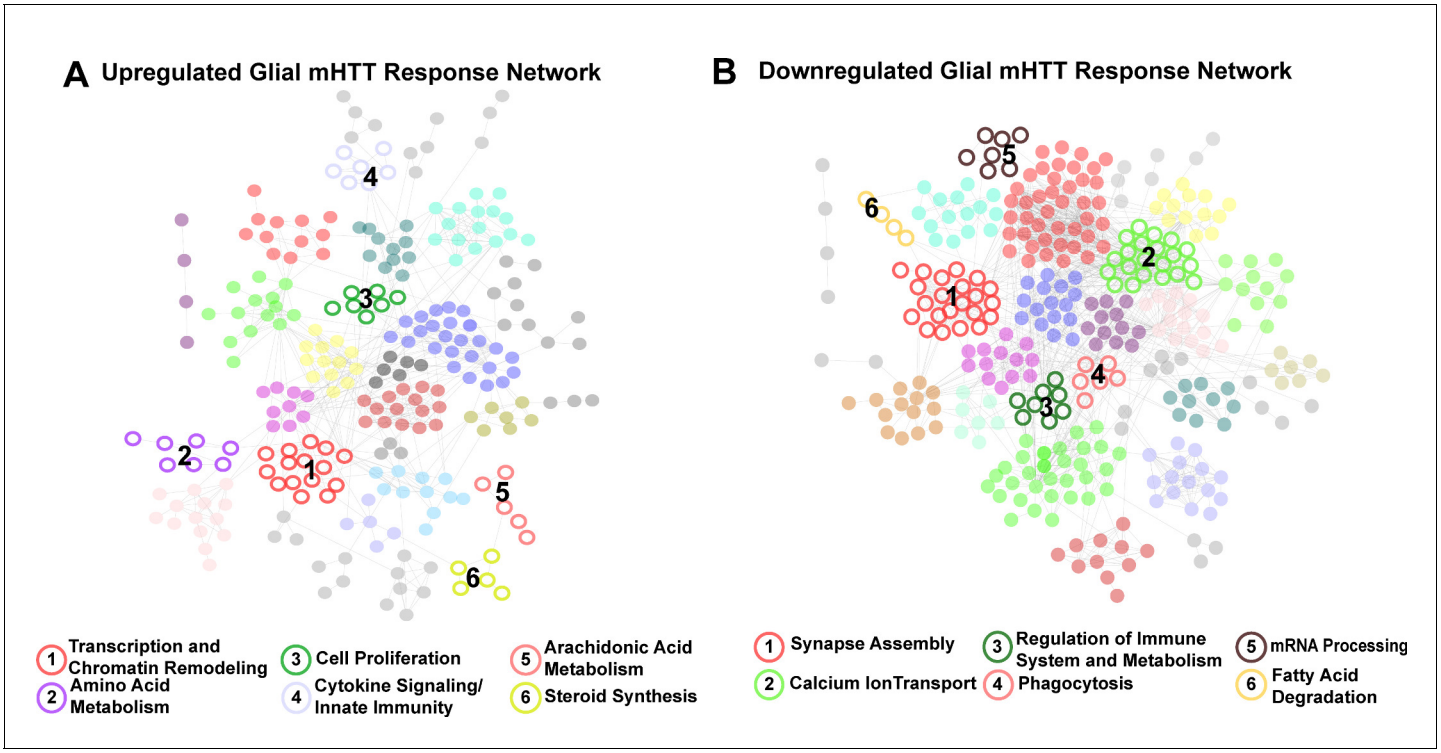

Figure 2. Clusters of concordant differentially expressed genes (DEGs) between human and mouse Huntington's disease (HD) striata and *Drosophila* expressing mutant Huntingtin (mHTT) in glia. Clustered protein-protein interaction (PPI) networks of DEGs (STRING-db) that have higher (**A**) or lower (**B**) concordant expression in HD human tissue, an allelic series of knock-in HD mouse models, and *Drosophila* expressing m*HTT* ($HTT^{NT231Q128}$ or HTT^{FLQ200}) in glia. Clusters of DEGs (nodes) that were dysregulated in response to m*HTT* expression in glia are numbered and represented by open circles. Annotations listed below each network correspond to each numbered cluster and represent a synthesis of the top five most significantly enriched GO Panther Biological processes and Kyoto Encyclopedia of Genes and Genomes (KEGG) terms with a false discovery rate (FDR) < 0.05 (***Supplementary file 2***). Nodes represented by solid circles were dysregulated in response to m*HTT* expression in glia but are also significantly similar in gene membership to clusters of DEGs in response to m*HTT* expression in neurons (***Figure 2—figure supplement 1***, hypergeometric test, $p<1\times10^{-5}$).

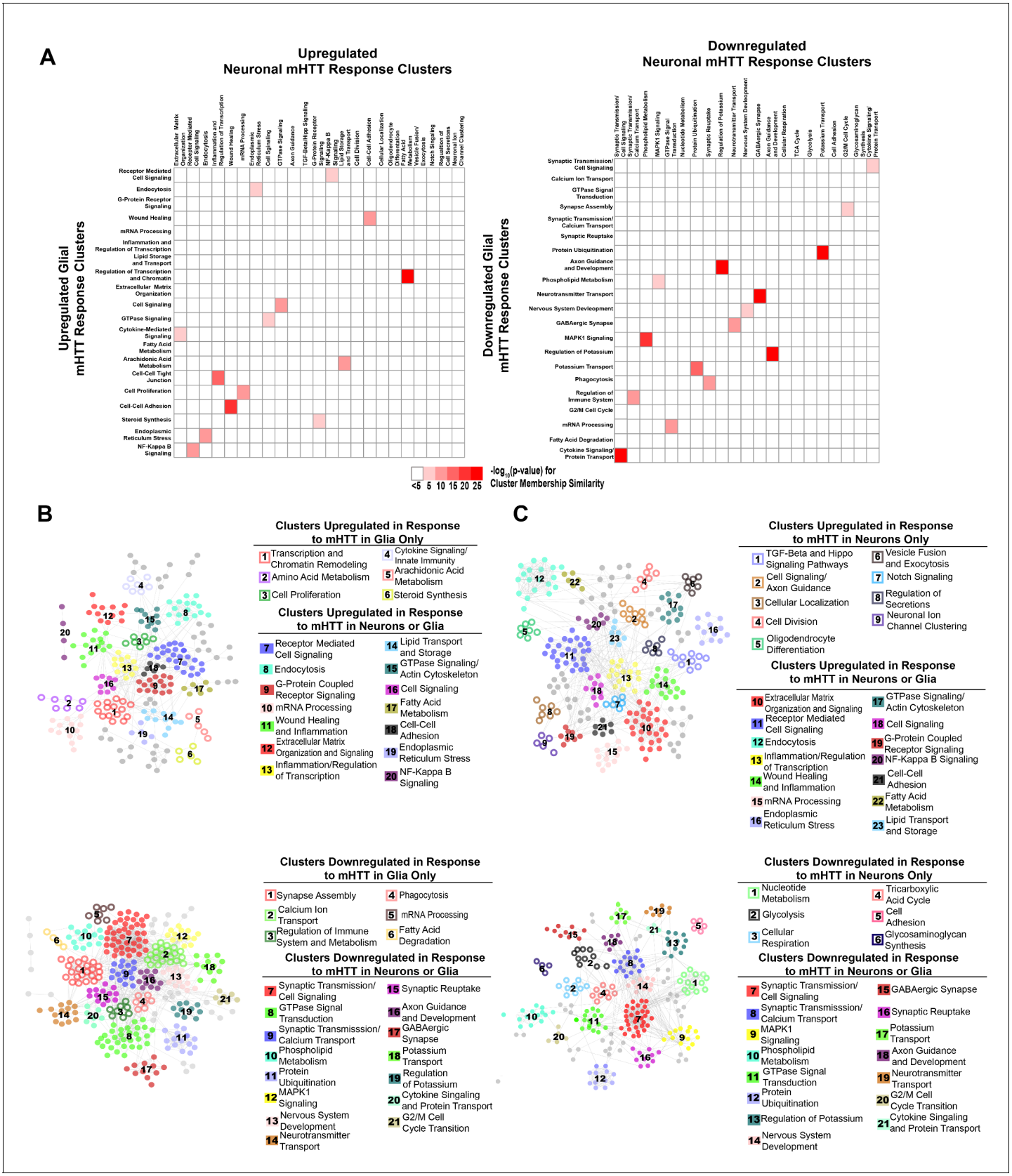

Figure 2—figure supplement 1. Network of differentially expressed genes (DEGs) responding concordantly to mutant *Huntingtin* (m*HTT*) expression in glia or neurons. (**A**) Heatmap representing all pairwise comparisons between clusters of upregulated (left) and downregulated (right) DEGs in response

Figure 2—figure supplement 1 continued on next page

Figure 2—figure supplement 1 continued

to glial (x-axis) or neuronal (y-axis) m*HTT* expression. Clusters are labeled using annotations for biological processes represented by DEGs within each cluster (refer to ***Supplementary file 3***). Color is scaled to represent the significance of membership similarity calculated using a hypergeometric distribution. Colors represent the -$\log_{10}$(p-value) and range from white (<5) to dark red (>25). (**B**) Protein-protein interaction (PPI) network (STRING-db) of upregulated (top) and downregulated (bottom) DEGs in human Huntington's disease (HD) tissue, HD mouse models, and *Drosophila* expressing m*HTT* in glia. (**C**) PPI network (STRING-db) of upregulated (top) and downregulated (bottom) DEGs in human HD tissue, HD mouse models, and *Drosophila* expressing m*HTT* in neurons. Refer to ***Supplementary file 3*** for gene membership, as well as GO Panther and KEGG terms enriched genes within each cluster. Numbers in (**B**) and (**C**) correspond to annotations. Hollow circles correspond to clusters of DEGs that are dysregulated in response to m*HTT* (*HTT*^{FLQ200} or *HTT*^{NT231Q128}) expression in only glia (*repo-GAL4*) or neurons (*elav-GAL4*). Solid circles correspond to clusters of DEGs that are dysregulated in response to m*HTT* expression in neurons or glia.

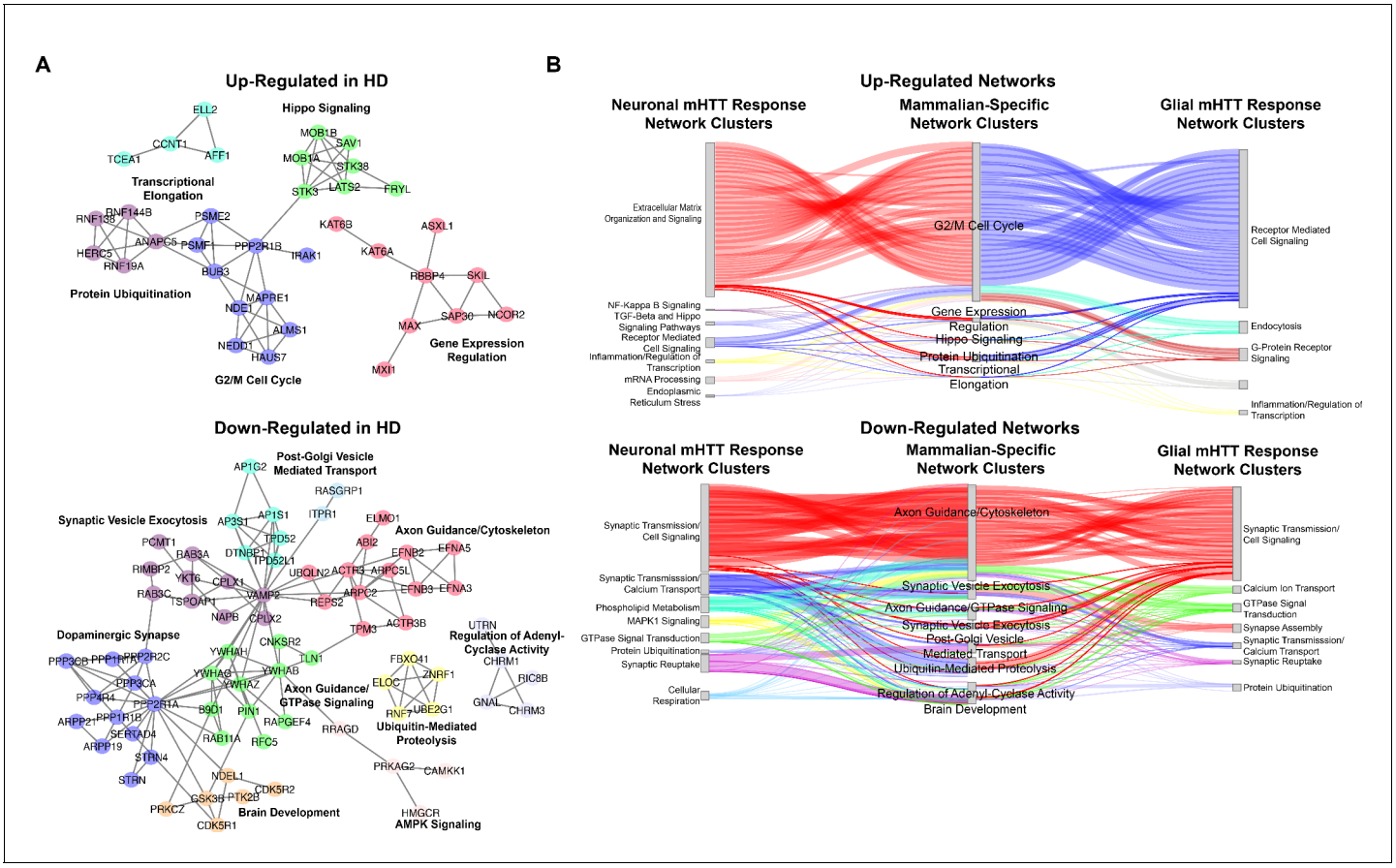

Figure 2—figure supplement 2. Network of differentially expressed genes (DEGs) concordantly altered in human Huntington's disease (HD) tissue and HD mouse models, but not in *Drosophila* HD models. (**A**) Clustered, annotated protein-protein interaction (PPI) network (STRING-db) of DEGs concordantly upregulated (top) and downregulated (down) in human HD striatal tissue collected post-mortem (***Hodges et al., 2006***) and the allelic series of knock-in HD mouse models (***Langfelder et al., 2016***), but not in the *Drosophila* models (this study). Clusters are annotated for the synthesis of the top five most significantly enriched GO Panther Biological Process and Kyoto Encyclopedia of Genes and Genomes (KEGG) terms (false discovery rate [FDR] < 0.05). (**B**) Sankey plot for genes concordantly upregulated (top) and upregulated (bottom) in HD patients and mouse model only (middle) connecting to cluster of DEGs that are concordantly upregulated in patients, mice, and *Drosophila* as a consequence of expressing mutant *Huntingtin* (*mHTT*) (*HTT*^{FLQ200} or *HTT*^{NT231Q128}) in neurons (*elav*) (left) or in glia (*repo*) (right). Edges represent PPIs between connected DEGs (STRING-db).

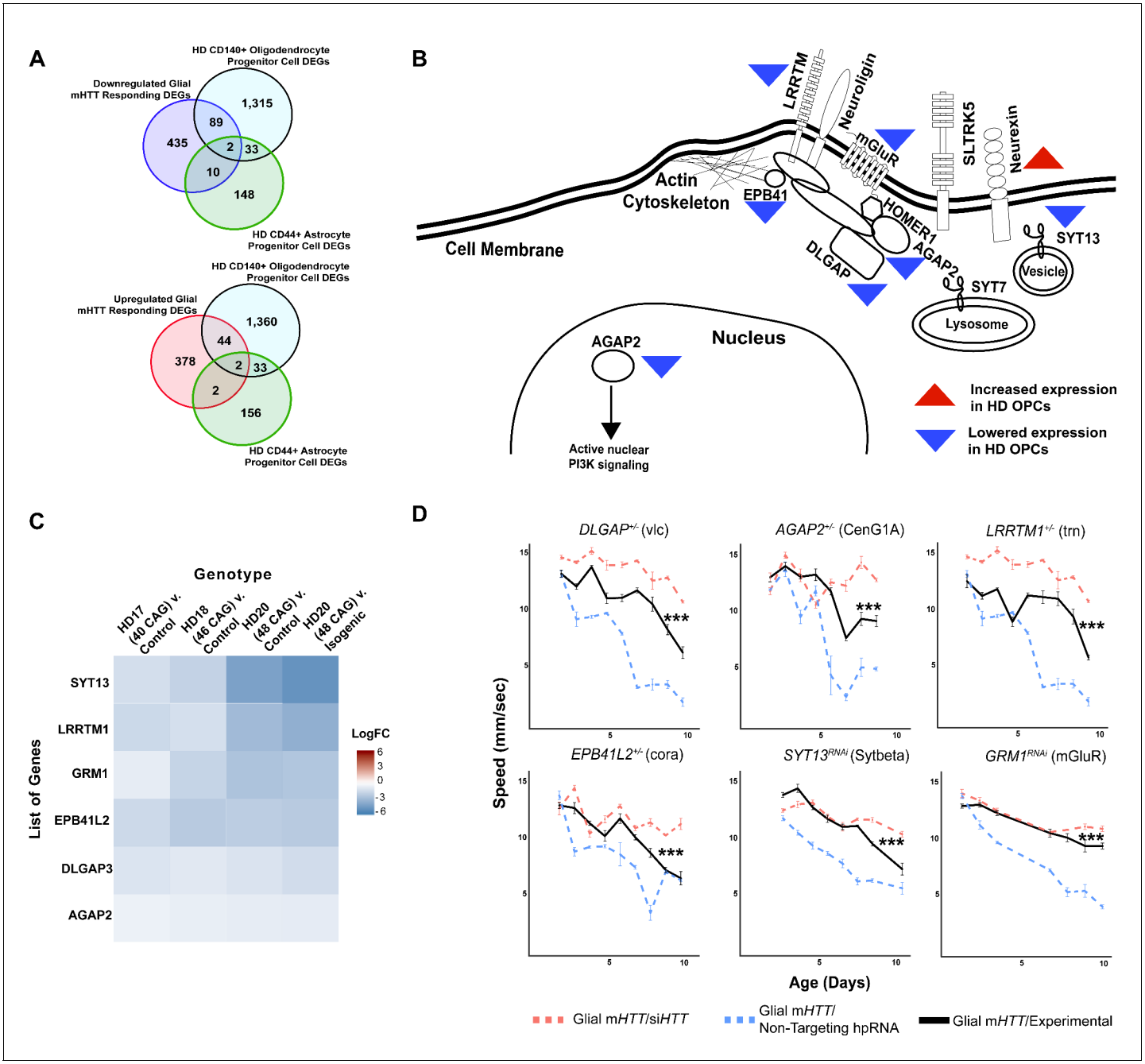

Figure 3. Reducing the expression of Synapse Assembly cluster genes in glia mitigates mutant Huntingtin (mHTT)-induced behavioral impairments. (**A**) Overlaps between concordant differentially expressed genes (DEGs) from the cross-species analysis defined as responding to m*HTT* expression in glia and DEGs identified in Huntington's disease (HD) human embryonic stem cells (hESCs) that have been differentiated into either CD140 + oligodendrocyte progenitor cells (OPCs) or CD44+ astrocyte progenitor cells (APCs) (***Osipovitch et al., 2019***). (**B**) Model placing Synapse Assembly cluster proteins into cellular context. The Synapse Assembly cluster was significantly enriched for DEGs in HD OPCs (Fisher's exact test, $p<0.001$). Only one gene, *NRXN3*, was upregulated in HD OPCs compared to controls (upward red triangle); the rest (*AGAP2*, *GRM1*, *LRRTM1*, *EPB41L2*, *DLGAP3*, and *SYT13*) were downregulated (downward blue triangles). (**C**) Heatmap representing genes with lower expression in HD OPCs compared to controls (presented as LogFC) that belong to the Synapse Assembly cluster. Each row is one downregulated gene; each column is a different HD human embryonic stem cell line, with CAG repeat length ranging from 40 to 48, compared to respective controls (***Osipovitch et al., 2019***). (**D**) Behavioral assessment of fruit flies that express m*HTT* only in glia, after reducing the expression of the overlapping DEGs in HD OPCs and the Synapse Assembly cluster. Plots show climbing speed as a function of age. ***$p<0.001$ between positive control and experimental (by linear mixed effects model and post-hoc pairwise comparison; see Materials and methods). Points and error bars on the plot represent the mean ± SEM of the speed for three technical replicates. Each genotype was tested with 4–6 replicates of 10 animals. Modifying alleles in (**D**) are listed in the Key resources table. Additional

Figure 3 continued on next page

Figure 3 continued

climbing data for these genes can be found in ***Figure 3—figure supplement 1A,*** and a summary of statistical analysis for this data can be found in ***Supplementary file 4***. Control climbing data for these alleles can be found in ***Figure 3—figure supplement 1B***. *Drosophila* genotypes: positive control (*w^{1118};UAS- non-targeting hpRNA/+; repo-GAL4,UAS-$HTT^{NT231Q128}$/+*), treatment control (*w^{1118}; repo-GAL4,UAS- $HTT^{NT231Q128}$/UAS-siHTT*), and experimental (*w^{1118}; repo-GAL4,UAS- $HTT^{NT231Q128}$/modifier*).

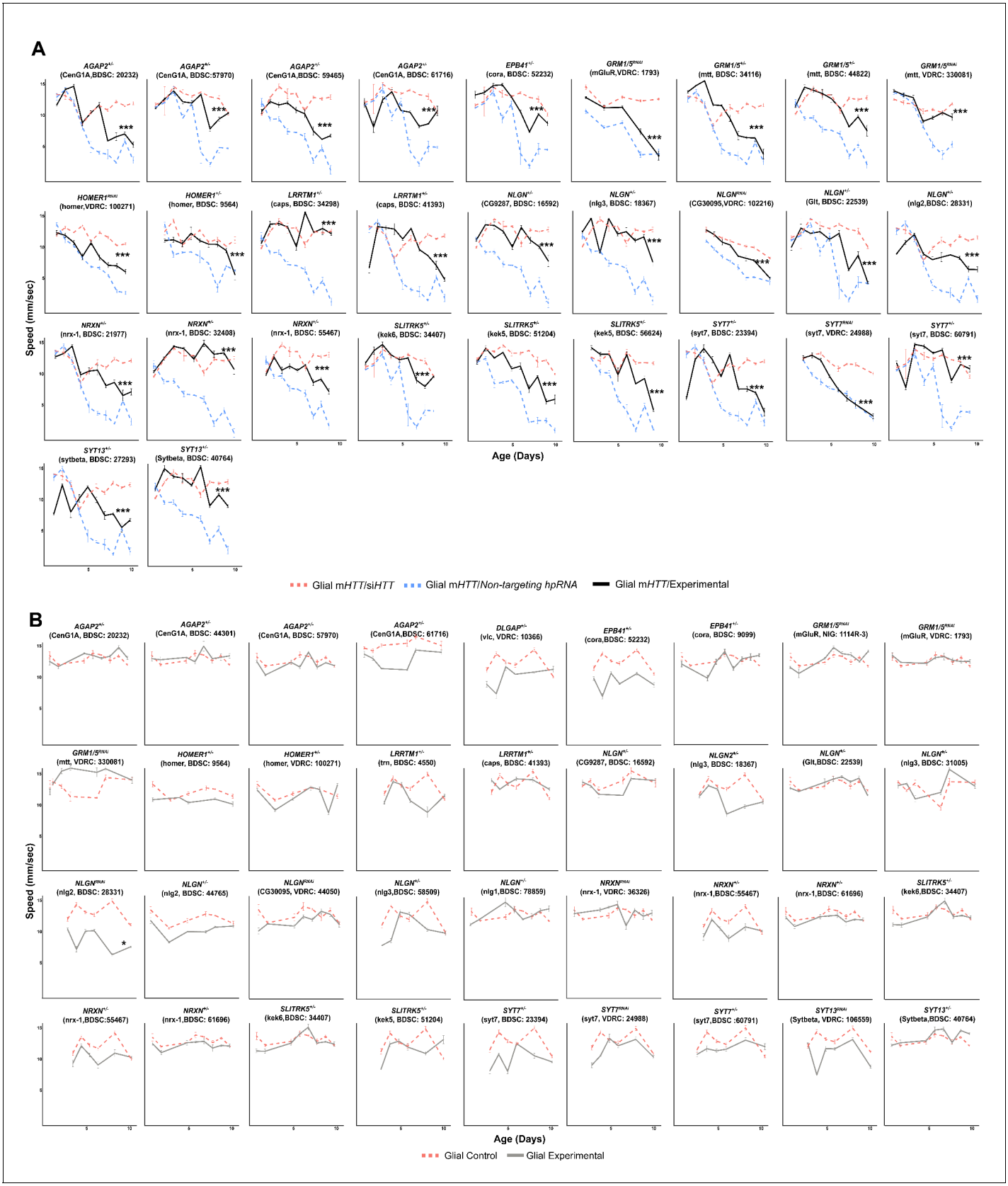

Figure 3—figure supplement 1. Suppressors of glial mutant Huntingtin (mHTT)-induced behavioral impairments among differentially expressed genes (DEGs) in the Synapse Assembly cluster. (**A**) Representative graphs of behavioral assays (climbing speed as a function of time) of *Drosophila*

Figure 3—figure supplement 1 continued on next page

Figure 3—figure supplement 1 continued

expressing m*HTT* in glia (*repo >HTTNT*^{NT231Q128}) and alleles knocking down genes in the Synapse Assembly cluster. ***p<0.001 between the positive control (dashed blue line) and experimental allele (solid black line) by linear mixed effects model and post-hoc, pairwise analysis (see Materials and methods). Refer to ***Supplementary file 4*** for a summary of the full statistical analysis. (**B**) Representative graphs of the climbing speed of wildtype *Drosophila* as a function of time with the glial driver (*repo-GAL4*) expressing alleles that suppress glial mHTT-induced behavioral impairments. Points and error bars on the plot represent the mean speed ± SEM of three technical replicates. Each experimental genotype was tested with 4–6 replicates of 10 animals. The gray line represents climbing speed of animals expressing the modifier allele in the *repo-GAL4* background. *Drosophila* genotypes: positive control (w^{1118}*/+;UAS- non-targeting hpRNA/+; repo-GAL4,UAS-* HTT^{NT231Q128}*/+*), treatment control (w^{1118}*; repo-GAL4,UAS-HTT*^{NT231Q128}*/UAS-siHTT*), experimental (w^{1118}*; repo-GAL4,UAS- HTT*^{NT231Q128}*/modifier*), negative control (w^{1118}*; UAS- non-targeting hpRNA/+; repo-GAL4/+*), and experimental control (w^{1118}*; repo-GAL4/modifier*).

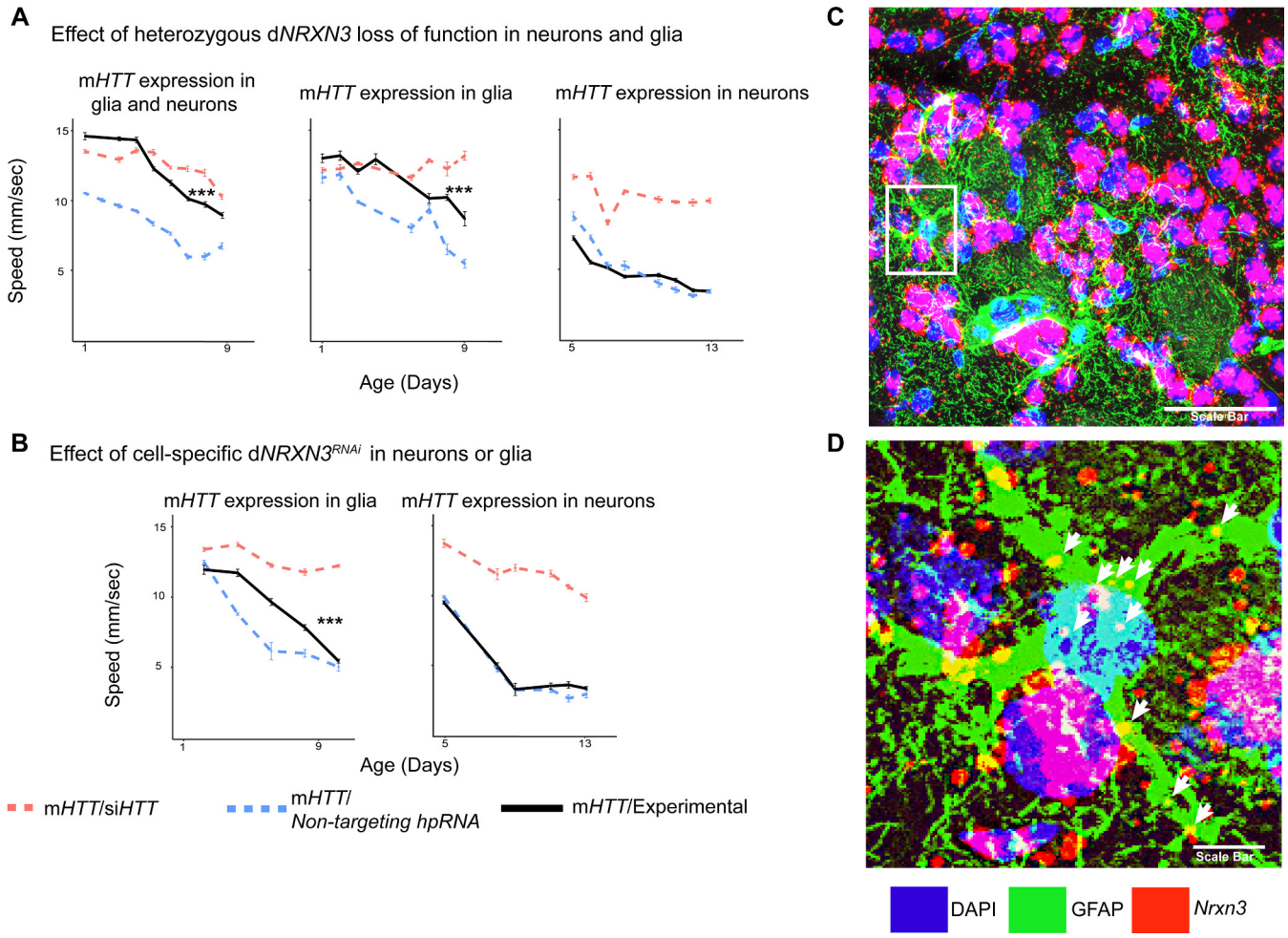

Figure 4. Glia-specific d*NRXN3* knockdown mitigates impairments caused by mutant *Huntingtin* (m*HTT*) expression. (**A**) Behavioral assays (climbing speed as a function of age) showing that d*NRXN3* heterozygous loss of function (LOF) ameliorates behavioral impairments caused by expression of m*HTT* in both neurons and glia and in glia alone, but not in neurons alone. (**B**) Glia-specific d*NRXN3* knockdown mitigates behavioral impairments caused by m*HTT* expressed solely in glia; however, neuron-specific knockdown of *dNRXN3* does not affect impairments induced by m*HTT* expressed solely in neurons. ***p<0.001 between positive control and experimental by linear mixed effects model and post-hoc pairwise comparison (see Materials and methods). Points and error bars on the plot represent the mean ± SEM of the speed for three technical replicates. Each genotype was tested with 4–6 replicates of 10 animals. A full summary of the statistical analysis for this data can be found in ***Supplementary file 4***. Control climbing data for these alleles can be found in ***Figure 3—figure supplement 1B***. (**C**) Astrocytes in the striatum of 6-month-old knock-in HD mice ($Hdh^{zQ175/+}$) expressing *Nrxn3*. In situ probe for *Nrxn3* mRNA is in red (appears magenta when overlapping with the DAPI channel), astrocytes are immunostained using an antibody specific for glial fibrillary acidic protein (GFAP) in green, and DAPI in blue. Image was taken at ×63 magnification using a Leica SP8 confocal microscope. Scale bar (in white on the bottom right) represents 50 µm. 3/5 (60%) of astrocytes in this field appear *Nrxn3* positive. (**D**) Magnified image of the astrocyte highlighted in the white box in (**C**). White arrows indicate yellow puncta where *Nrxn3* mRNA localizes to astrocytes. Scale bar (in white on the bottom right) represents 5 µm. See ***Figure 4—figure supplement 1*** for additional images and quantification of *Nrxn3* in situ signal in striatal astrocytes in $Hdh^{zQ175/+}$ mice. *Drosophila* genotypes: *dNRXN3* LOF allele (y^1 *w*; Mi{*$y^{+mDint2}$*=MIC}nrx-1*^{MI02579}or *nrx-1*^{LOF}, BDSC: 61696), dNRXN3 RNAi allele (*UAS-nrx-1*^{hpRNA}, VDRC: 36326), neuronal and glial Huntington's disease (HD) model with d*NRXN3* mutant (*elav*^{c155}*-GAL4/* y^1 *w*; repo-GAL4,UAS-HTT*^{NT231Q128}*/Experimental allele*), glial HD model with d*NRXN3* mutant (w^{1118}/y^1 *w*; repo-GAL4,UAS-HTT*^{NT231Q128}*/ Experimental allele*), and neuronal model with dNRXN3 mutant (*elav*^{c155}*-GAL4/*y^1 *w*; UAS-HTT*^{NT231Q128}*/Experimental allele).*

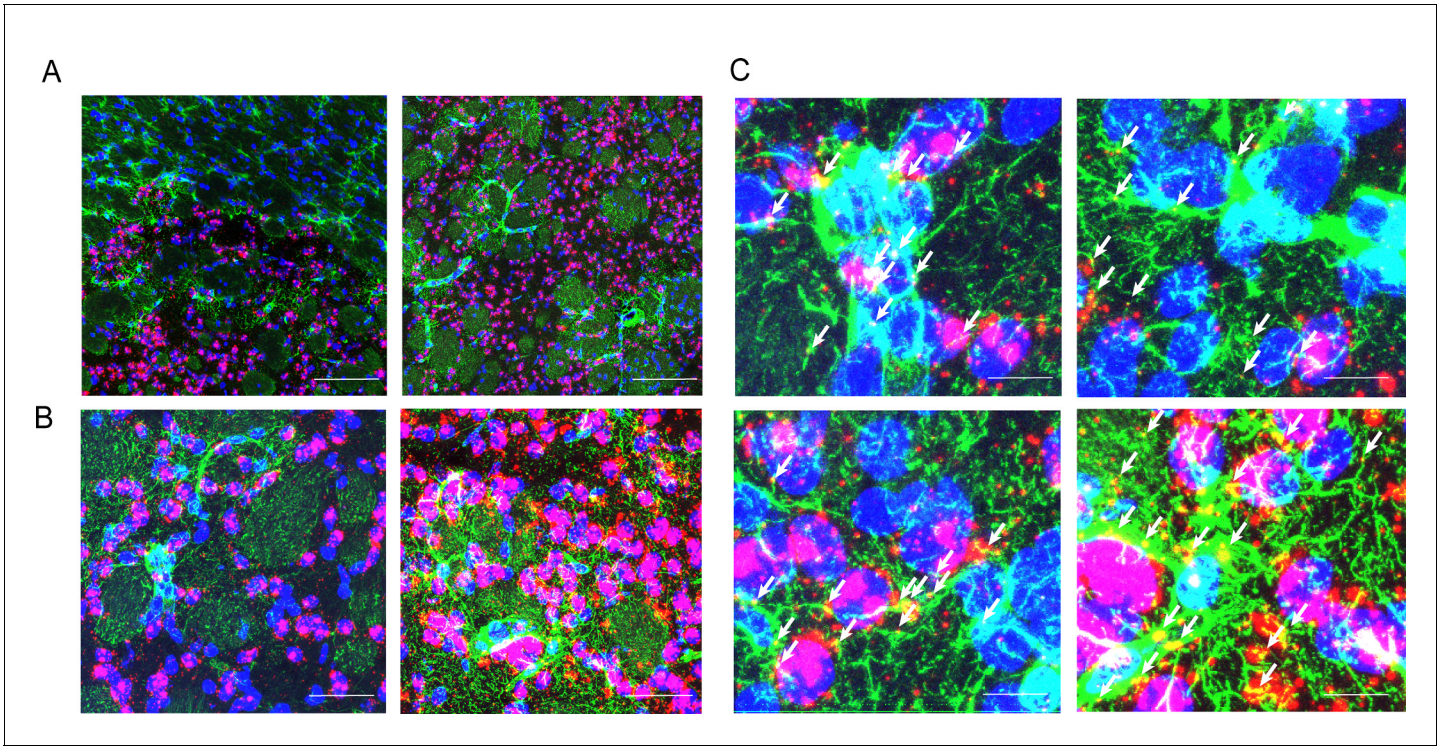

Figure 4—figure supplement 1. Additional images of astrocytes expressing *Nrxn3* in the striatum of *Hdh*$^{zQ175/+}$ mice and quantification. Astrocytes in the striatum of 6-month-old knock-in Huntington's disease (HD) mice (*Hdh*$^{zQ175/+}$) expressing *Nrxn3*. In situ probe for *Nrxn3* mRNA is in red (appears magenta when overlapping with the DAPI channel), astrocytes are immunostained using an antibody specific for glial fibrillary acidic protein (GFAP) in green, and DAPI in blue. Images were taken at ×20 (**A**) and ×63 (**B**) magnification using a Leica SP8 confocal microscope. 10/22 (45.5%) astrocytes were clearly *Nrxn3* positive. In digitally magnified images in (**C**), white arrows highlight localization of anti-GFAP and *Nrxn3* mRNA staining.

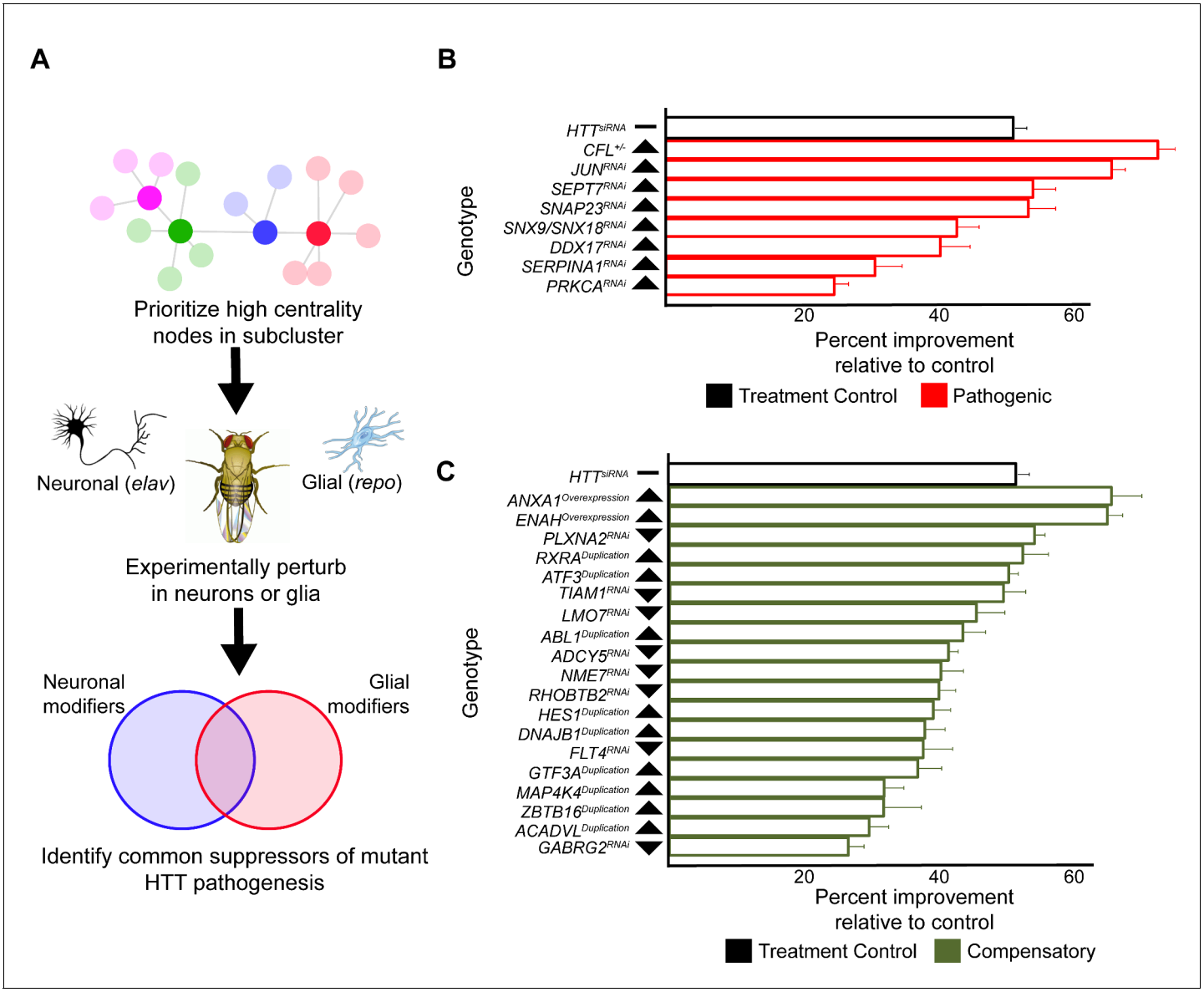

Figure 5. Compensatory and pathogenic gene expression changes shared by neurons and glia in response to mutant *Huntingtin* (m*HTT*) expression. (**A**) Our approach for identifying modifiers of mHTT-induced behavioral impairments common to both neurons and glia. Genes that were central to their respective clusters were prioritized and manipulated in *Drosophila* expressing m*HTT* ($HTT^{NT231Q128}$) in either neurons (*elav-GAL4*) or glia (*repo-GAL4*). (**B**) Red bars represent the percent improvement in behavior over a 9-day trial compared to positive control (non-targeting hpRNA) in *Drosophila* expressing *mHTT* in neurons and glia, after we antagonized pathogenic gene expression changes. (**C**) Green bars represent the percent improvement in behavior over a 9-day trial compared to control (see **B**), after we mimicked compensatory gene expression alterations. In (**B**) and (**C**), the top black bars represent the effect of directly targeting the m*HTT* transgene using a small interfering RNA (siRNA). Arrowheads indicate the direction of the conserved, concordant altered expression for each gene as a result of m*HTT* expression in humans, mice, and *Drosophila*. Behavioral assay graphs corresponding to the data presented in (**B**) and (**C**) can be found in ***Figure 5—figure supplement 1A***. Corresponding statistical analysis for (**B**) and (**C**) can be found in ***Supplementary file 6***. Corresponding controls for behavioral data can be found in ***Figure 5—figure supplement 1B, C***. *Drosophila* genotypes: positive control ($elav^{c155}$-*GAL4*/w^{1118};*UAS- non-targeting hpRNA/+; repo-GAL4,UAS-*$HTT^{NT231Q128}$/+), treatment control ($elav^{c155}$-*GAL4*/w^{1118}; *repo-GAL4, UAS-* $HTT^{NT231Q128}$/*UAS-siHTT*), and experimental ($elav^{c155}$-*GAL4*/w^{1118}; *repo-GAL4, UAS-* $HTT^{NT231Q128}$/*modifier*).

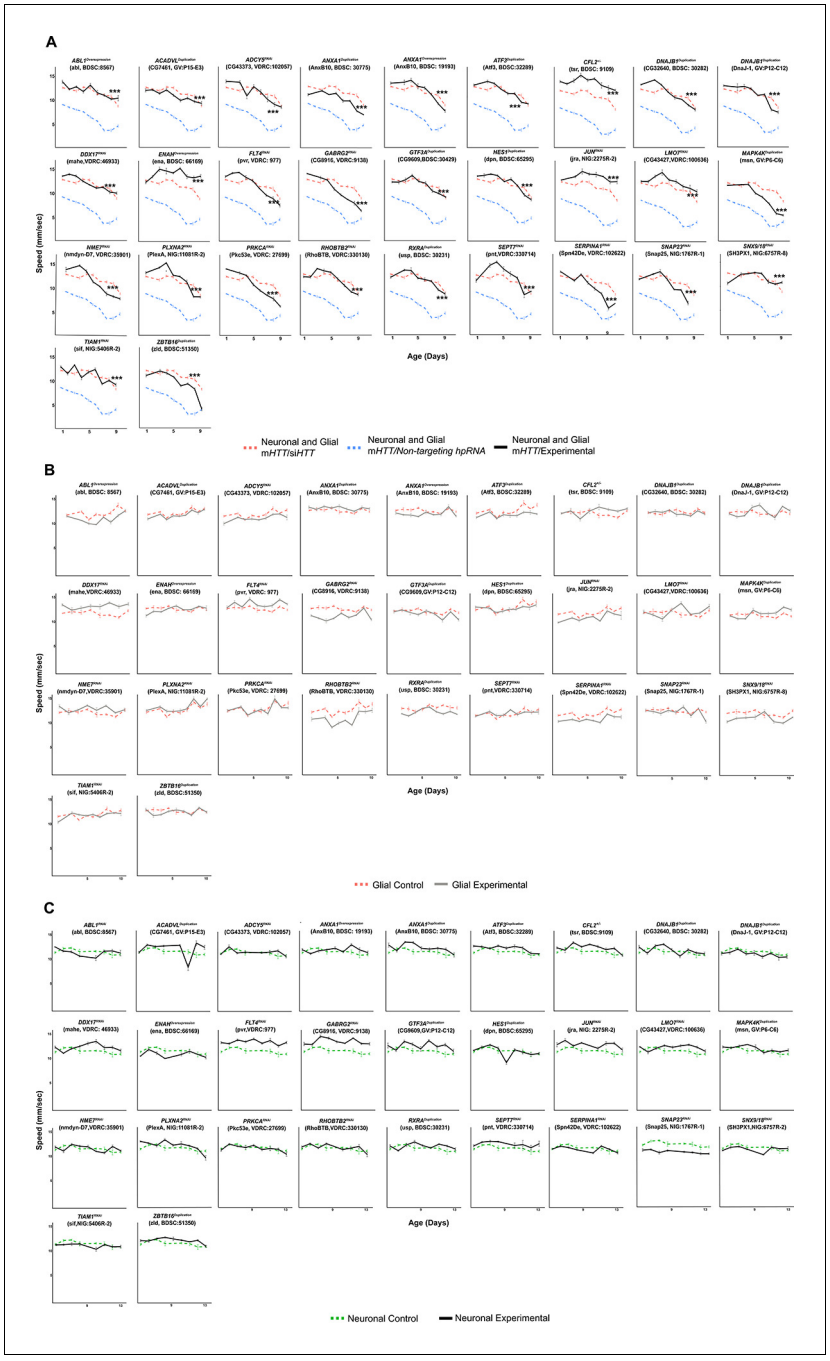

Figure 5—figure supplement 1. Genetic modifiers suppress behavioral impairments caused by mutant *Huntingtin* (m*HTT*) expression in neurons and glia. (**A**) Representative graphs of the climbing speed of animals expressing mutant HTT in neurons and glia in combination with common modifiers as a function of time. ***p<0.001 between the positive control (dashed blue line) and experimental allele (solid black line) by linear mixed effects model and post-hoc, pairwise analysis. Refer to ***Supplementary file 6*** for full statistical analysis of each genotype in neurons, glia, and both. (**B**) Representative graphs of the speed of wildtype *Drosophila* with the glial driver (*repo-GAL4*) and alleles that suppressed mutant HTT-induced behavioral impairments in both neurons and glia. The dashed red line represents the longitudinal climbing speed of animals expressing a non-targeting hpRNA in glia, while the gray line represents climbing speed of animals expressing the common modifier allele in the *repo-GAL4* background. (**C**) Representative graphs of the speed of wildtype *Drosophila* with the neuronal driver (*elav-GAL4*) expressing the alleles that suppressed mutant HTT-induced behavioral impairments in both neurons and glia as a function of time. The dashed green line represents the climbing speed of animals

Figure 5—figure supplement 1 continued on next page

Figure 5—figure supplement 1 continued

expressing a non-targeting hpRNA in neurons, while the black line represents climbing speed of animals expressing the common modifier allele in the *elav-GAL4* background. Points and error bars on the plot represent the mean speed ± SEM of three replicates. Each genotype was tested with 4–6 replicates of 10 animals. *Drosophila* genotypes: neuronal and glial mHTT positive control (*elav^{c155}-GAL4/w^{1118};UAS-non-targeting hpRNA/+; repo-GAL4, UAS- HTT^{NT231Q128}*/+), neuronal and glial mHTT treatment control (*elav^{c155}-GAL4/w^{1118}; repo-GAL4, UAS-HTT^{NT231Q128}/UAS-siHTT*), neuronal and glial experimental (*elav^{c155}-GAL4/w^{1118}; repo-GAL4, UAS- HTT^{NT231Q128}/modifier*), glial control (*elav^{c155}-GAL4/w^{1118}; UAS-non-targeting hpRNA/+*), glial experimental control (*elav^{c155}-GAL4/w^{1118}; modifier/+*), neuronal control (*w^{1118}; UAS-non-targeting hpRNA/+; repo-GAL4/+*), and neuronal experimental control (*w^{1118}; repo-GAL4/modifier*).

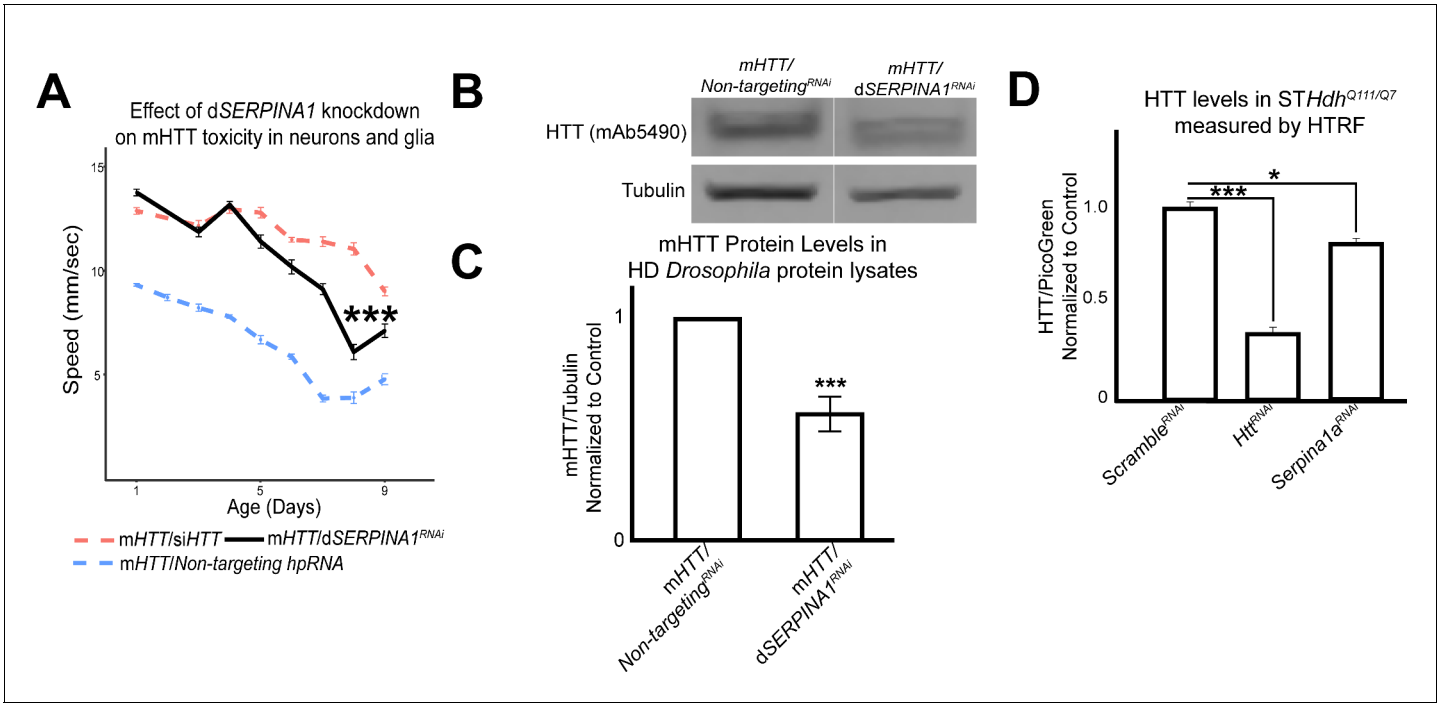

Figure 6. Antagonizing the pathogenic overexpression of *SERPINA1* in neurons and glia mitigates mutant *Huntingtin* (mHTT)-induced behavioral impairments and lowers mHTT protein levels in *Drosophila* and Huntington's disease (HD) mouse striatal cells. (**A**) Behavioral assays following knockdown of *dSERPINA1* in *Drosophila* expressing m*HTT* in neurons and glia. *** indicates p<0.001 by linear mixed effects model and post-hoc pairwise comparison between positive control and experimental animals. Points and error bars on the plot represent the mean ± SEM of three technical replicates. Each genotype was tested with 4–6 replicates of 10 animals. (**B**) Representative western blot showing lower levels of mHTT following knockdown of *dSERPINA1* in *Drosophila* expressing m*HTT* in neurons and glia. (**C**) Quantification of five independent immunoblots showing the effect of *dSERPINA1* knockdown on mHTT levels in *Drosophila* head protein lysates. ***p<0.001 between positive control and d*SERPINA1* knockdown by one-way t-test. (**D**) Quantification of HTT protein levels in HD mouse striatal-derived cells (ST*Hdh*$^{Q111/Q7}$) measured by homogenous time-resolved fluorescence (HTRF) following treatment with a pool of scramble small interfering RNAs (siRNAs) (negative control), a pool of siRNAs against *Htt*, and a pool of siRNAs against *Serpina1a*. Quantification is presented as a ratio of the emission signal from the fluorescent D2 dye (HTT)/PicoGreen (number of cells per well). n = 9 for each treatment group. *p<0.05 and ***p<0.001 between genotypes by Fisher's Least Significant Difference (LSD) test. *Drosophila* genotypes: *dSERPINA1* RNAi allele (*UAS-Spn42De*^{hpRNA}, VDRC: 102622), positive control (*elav*^{c155}*-GAL4/w*^{1118}*;UAS- non-targeting hpRNA/+; repo-GAL4,UAS-HTT*^{NT231Q128}*/+*), treatment control (*elav*^{c155}*-GAL4/w*^{1118}*; repo-GAL4, UAS- HTT*^{NT231Q128}*/UAS-siHTT*), and dSERPINA1 experimental (*elav*^{c155}*-GAL4/w*^{1118}*;UAS-Spn42De*^{hpRNA}*/+; repo-GAL4, UAS-HTT*^{NT231Q128}*/+*).

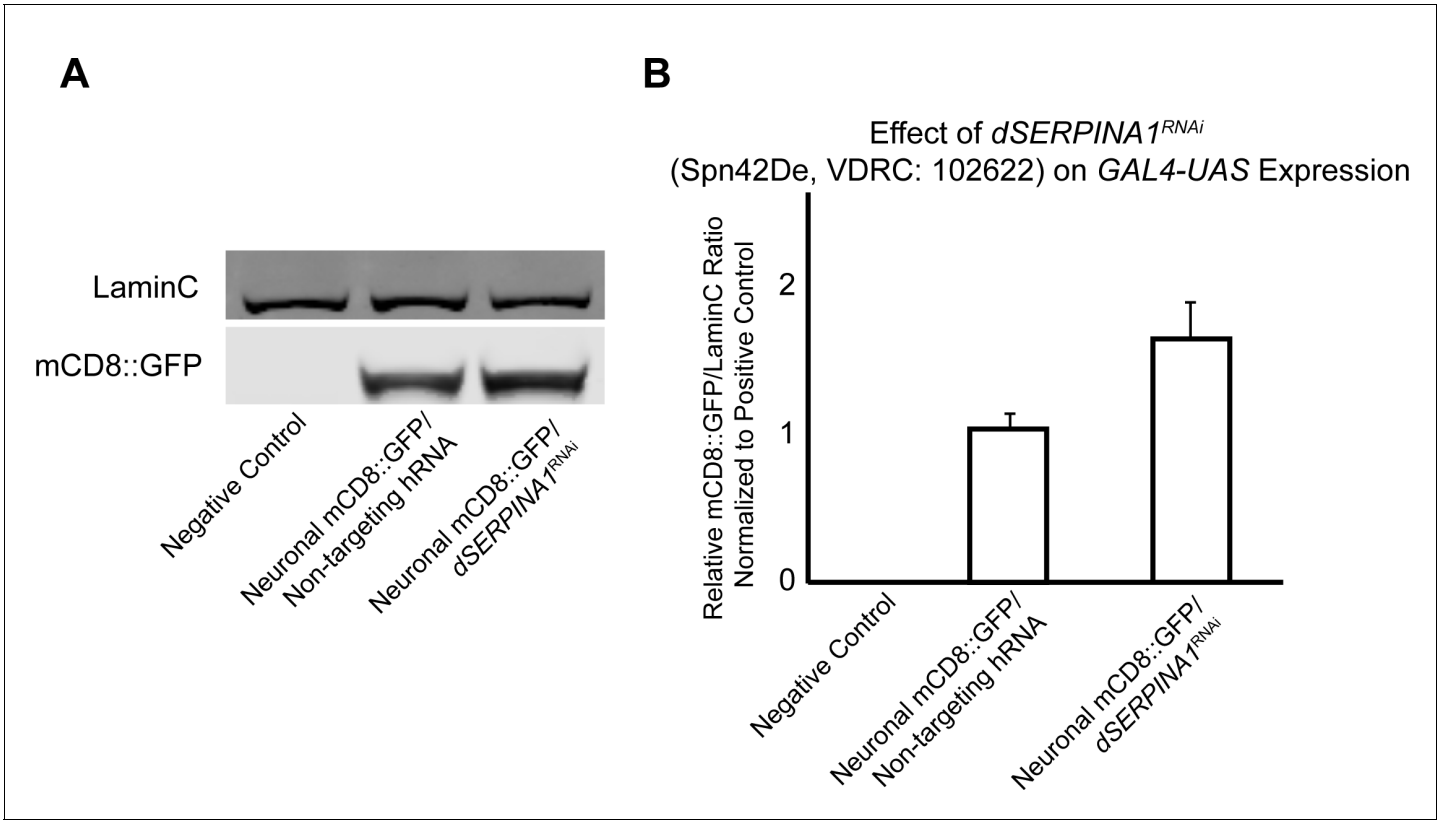

Figure 6—figure supplement 1. d*SERPINA1* knockdown does not reduce the expression of the *GAL4-UAS* system. (**A**) Representative immunoblot performed on *Drosophila* protein lysates assessing mCD8::GFP protein levels as a proxy for *GAL4-UAS* expression. *mCD8::GFP* was expressed in neurons using the *elav-GAL4* driver. The negative control in this experiment was *elav >GAL4* driving the expression of a non-targeting hpRNA (left lane). The positive control was *elav >GAL4* expressing the *mCD8::GFP* construct and a non-targeting hpRNA (middle lane). The experimental was *elav >GAL4* driving the expression of the *mCD8::GFP* construct and the d*SERPINA1*^{RNAi} (Spn42De, VDRC: 102622) allele that reduced mutant protein levels in ***Figure 6*** (right lane). LaminC was used as a loading control in this immunoblot. (**B**) Quantification of the three replicates from the immunoblot in (**A**) represented as the ratio of mCD8::GFP to LaminC, normalized to the average of the positive control (presented as mean ± SEM).

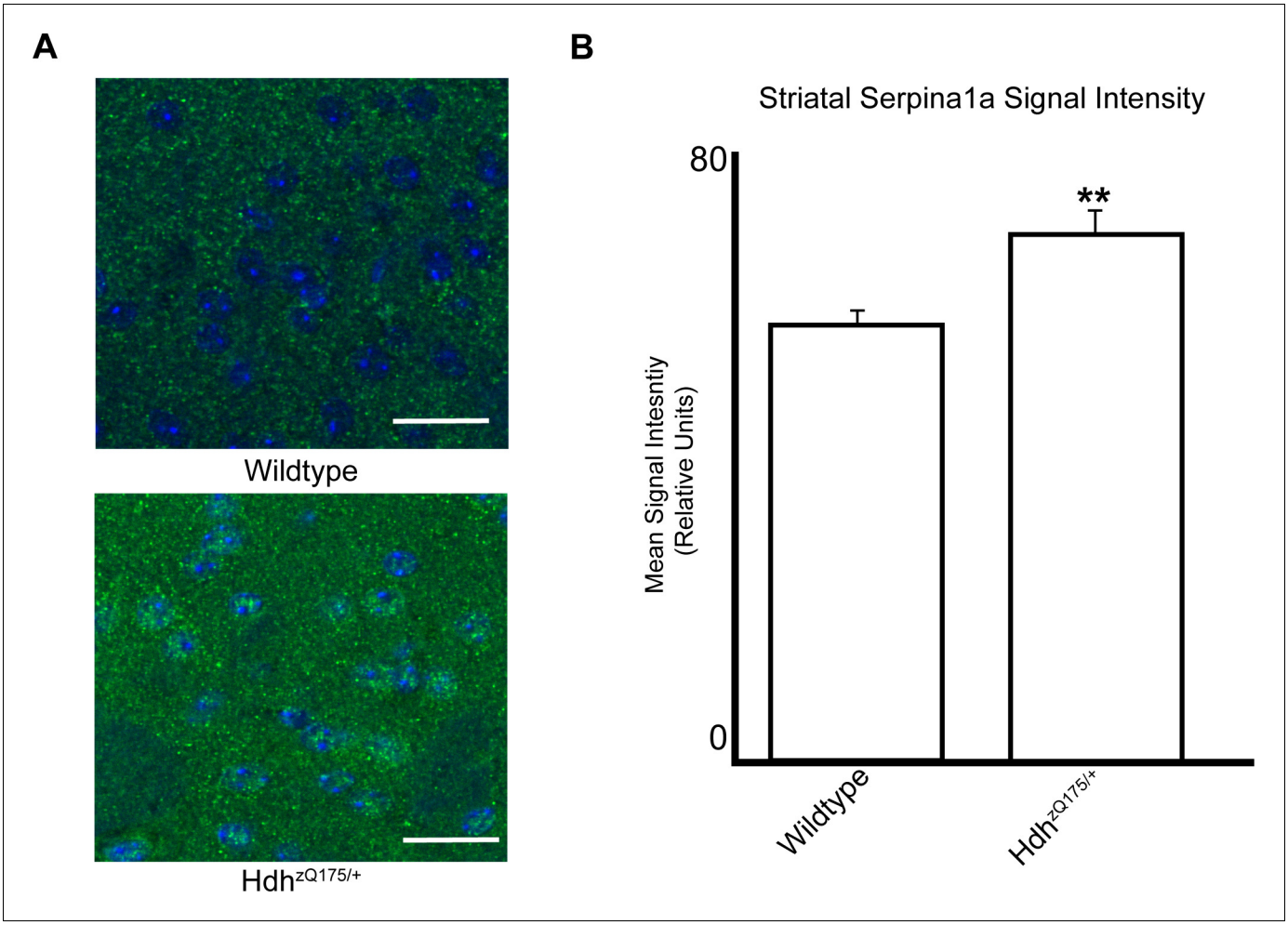

Figure 6—figure supplement 2. Serpina1a protein accumulates in the striata of *Hdh*$^{zQ175/+}$ mice compared to wildtype littermates. (**A**) Representative images of fixed, paraffin-embedded coronal brain slices at the striatum of *Hdh*$^{zQ175/+}$ and wildtype mice, stained with an antibody against Serpina1a (green). Images were taken on a Leica SP8 confocal microscope using a magnification of ×20 along with ×6.93 digital zoom. DAPI staining is in blue. (**B**) Quantification of measured mean signal intensity (presented as mean ± SEM) for Serpina1a, comparing *Hdh*$^{zQ175/+}$ and wildtype mice. ** indicates significant difference between the *Hdh*$^{zQ175/+}$ and wildtype mice by a two-way t-test assuming unequal variances (p=0.003). Statistical analysis and raw data are available in ***Figure 6—figure supplement 2—source data 1***.